

Synthesis, spectroscopic studies, antimicrobial activity and theoretical studies of 6-nitro-2-(4-nitrophenyl)-1H-benzimidazole.

¹ F. Liakath Ali Khan, ¹ Fasiuddin G S

¹Department of Physics, Islamiah College, Vaniyambadi-635752, Tamil Nadu, India.

Abstract : The synthesis of 6-nitro-2-(4-nitrophenyl)-1H-benzimidazole has been reported and characterized by FT-IR spectra in the region of 4000-400 cm⁻¹. UV-visible spectroscopy, ¹H NMR experimental techniques. The theoretical studies such as molecular structure parameter, vibrational frequencies, electronic absorption spectra has been investigated using gas and solvent phase, HOMO-LUMO, molecular electrostatic potential (MEP) and natural bond orbital (NBO), of the title compound has been computed using the HF and DFT (B3LYP, B3PW91) methods with 6-31+G (d, p) and 6-31++G (d, p) basis sets. ¹H –NMR Gauge Including Atomic Orbital (GIAO) chemical were calculated using 6-311++ G (d, p) basis set. The vibrational wavenumber and the chemical shifts values were compared with the obtained experimental data of the title compound. The electronic properties were evaluated by TD-DFT methodology in different solutions and in gas-phase method using integral equation formalism of the polarisable continuum model (IEF-PCM) at B3LYP/6-311++G (d, p) basis set. HOMO-LUMO energy band gap has been determined. The inter molecular electronic interaction and the stabilization energy was determined using NBO analysis. In addition to this the antimicrobial evaluation of 6-nitro-2-(4-nitrophenyl)-1H-benzimidazole was also performed against some bacteria and fungi using Disc – diffusion method. The inhibition zone of growth was also determined for bacterial and fungal strain.

Keywords: Benzimidazole, FT-IR, NMR, NBO, UV –Vis, DFT, Anti-microbial.

1. INTRODUCTION

Benzimidazole is one of the most significant and promising heterocyclic compound. It is the N-containing organic compound fused with benzene and imidazole. Benzimidazole has the wide range of biological and pharmacological activities [1-2]. It is present in various drugs compound such as astemizole, emedastine difumarate, mebendazole and omeprazole [3]. Benzimidazole moiety fulfils the structural requirement and the scientist from the worldwide have reported that the substitute compound have remarkable activity such as antiviral, anti-proliferative, anti-hypertensive, anthelmintic, human glucagon receptor, antagonist and anti-infective activities [4-9].

The substituted benzimidazole molecules have prodigious importance in drug discovery owing to their unique and precise binding abilities for the biological targets with respect to their chemical formalization [10]. Considering the above facts the intent of this study is to perform an experimental and computational work on benzimidazole fusing with aryl group. In this study we describe the vibrational frequencies, ¹H chemical shifts and excitation energies have been investigated on 6-Nitro-2-(4-nitrophenyl)-1H-benzimidazole. The optimized geometric parameters and vibrational frequencies have been calculated using HF method with basis sets 6-31+G (d, p), 6-311++G (d, p) and similarly with DFT methods (B3LYP, B3PW91) methods along with basis sets 6-31+G (d, p), 6-311++G (d, p). HOMO-LUMO analysis have also been investigated using TD-DFT/B3LYP the 6-311++G (d, p) basis set by applying the integral equation formalism of the polarizable continuum model (IEF-PCM) along with this molecular electrostatic potential (MEP) and natural bond analysis (NBO). In addition we report the evaluation of the antimicrobial activities.

2. MATERIALS AND METHODS

2.1 General

The compound 2-(4-nitrophenyl)-1H-benzimidazole was purchase from the Sigma Aldrich Company with a state of 98% purity. The three necked round bottom flask fitted with a mechanical stirrer was taken and 7.5 ml concentrated Nitric acid (HNO₃) was added. The flask was immersed in ice cold water and concentrated sulphuric acid (H₂SO₄) of 7.5 ml was added slowly down the condenser along stirring. The compound 2-(4-nitrophenyl)-1H-benzimidazole of 6.70 gm were added in a portion of 1 hour at such a rate that the temperature did not exceed 35°C. It is stirred continuously for 12 hour then the reaction mixture was poured very slowly over crushed ice with intense stirring. The obtained product was filtered, washed with cold water and recrystallized from ethanol [11-12]. The FT-IR spectrum of the compound was measured in the region of 4000 -400 cm⁻¹ using KBr pellets. A UV-vis spectrum was carried out in the wavelength region of 500- 200 nm. The ¹H nuclear magnetic resonance was recorded on Bruker advanced 500 NMR spectrometer.

2.2 Computational method

The theoretical calculations were carried out with GAUSSIAN 16W program packages [13]. The calculated results were visualized by means of Gauss view 6.0 [14]. In the present work we have calculated the vibrational frequencies and the geometric parameters of a 6-Nitro-2-(4-nitrophenyl)-1H-benzimidazole, in the ground state to compare the fundamentals from the experimental vibration frequencies and geometric parameters, by using the Hartree-Fock (HF) [15], Density functional theory using Becke's three parameter hybrid functionals [16] with Lee, Yang, and Parr correlation functional methods (B3LYP) [17], Becke's three parameter exchange functionals with Perdew-Wang exchange functional with Perdew and Wang's gradient correlated functional (B3PW91) [16-18] with the standard 6-31+G(d,p) and 6-311++G(d,p) basic sets. The optimized molecule structure is used for the computation of vibrational frequencies. The integral equation formalism –polarized continuum model (IEF-PCM) [19] dealing with solvent effect was selected in electronic transition calculation. ¹H and ¹³C NMR chemical shift values for 6-Nitro-2-(4-nitrophenyl)-1H-benzimidazole were computed by the same method in the solvent by using gauge-independent atomic orbital (GIAO). The IEF-PCM model provided by Gaussian 16W was used to evaluate the solvent

effects (chloroform, ethanol, DMSO). Along with this we also investigated the atomic charges, molecular electrostatic potential (MEP), Natural bond analysis (NBO) properties and HOMO-LUMO pictures were also obtained.

3. RESULTS AND DISCUSSION

3.1 Geometry optimization

The geometry optimization of the 6-Nitro-2-(4-nitrophenol)-1H-benzimidazole have been carried out using the HF and DFT (B3LYP/B3PW91) methods with the 6-31+G(d,p) and 6-311++G(d,p) basis sets. The title compound belongs to C₁ point group symmetry and the optimized geometric structure is shown in Fig 1, while the optimized structural parameters are presented in the Table 1. It is seen from the Table 1, most of the optimized bond lengths agree with each other for the three methods. The crystal data of closely related molecule [20-22] is compared with the title compound. The imine length is shorter than amine length as expected imine N6-C10 is 1.3178 and amine has 1.3807 as expected [20]. The bond length of O4-N8 and O3-N8 are almost equal to 1.23 Å [22]. The intra molecular C-C bond lengths are in range 1.38-1.40 Å except C10-C12 which is 1.464. The N6-C10-C12 and C21-N8-O4 bond angles of the title compound are 124.23° and 117.55° respectively. The highest bond angle of 132.58° was obtained for C13-C9-N5. The dihedral angle N6-C10-C12-C16 and C15-C13-C9-N5 are 179.99 and -179.99, respectively.

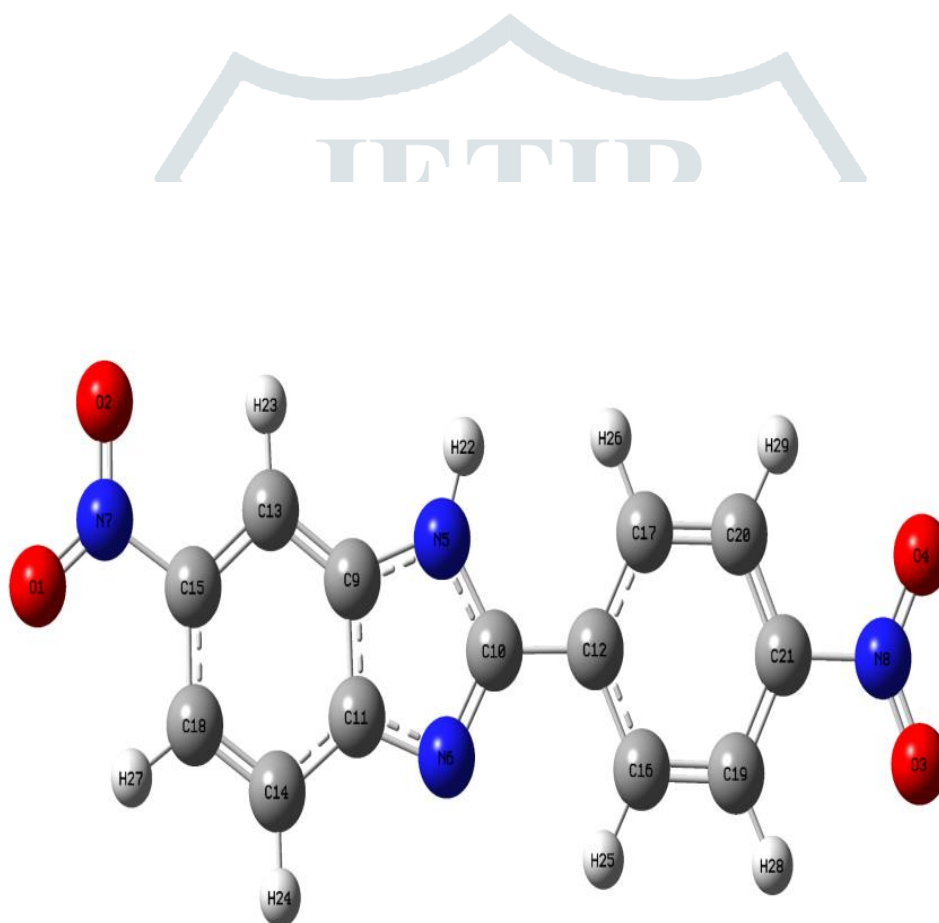


Fig 1. The optimized geometric structure of the molecule 6-Nitro -2-(4-nitrophenol)-1H-benzimidazole

Table 1: Optimized geometrical parameters of 6-Nitro-2-(4-nitrophenol)-1H-benzimidazole:
bond length (Å), bond angles (°) and selected dihedral angles (°)

Parameters	Exp. ^a	B3LYP 6311++ G (d, p)	B3PW91 6311++ G (d, p)	HF 6311++ G (d, p)	B3LYP 6311+ G (d, p)	B3PW91 6311+ G (d, p)	HF 6311+ G (d, p)
Bond length (Å)							
O1-N7	1.223	1.224	1.218	1.186	1.232	1.226	1.193
O2-N7	1.223	1.226	1.220	1.189	1.234	1.228	1.196
O3-N8	1.230	1.223	1.218	1.186	1.231	1.225	1.193
O4-N8	1.237	1.224	1.218	1.187	1.232	1.226	1.194
N7-C15	1.491	1.475	1.470	1.463	1.469	1.465	1.458
C15-C13	1.395	1.390	1.387	1.377	1.393	1.390	1.379
C15-C18	1.402	1.406	1.403	1.397	1.410	1.407	1.399
C18-H27	1.080	1.080	1.082	1.070	1.082	1.083	1.071
C18-C14	1.374	1.383	1.381	1.374	1.387	1.384	1.376
C14-C11	1.402	1.401	1.399	1.392	1.404	1.402	1.394
C11-N6	1.378	1.374	1.370	1.374	1.376	1.371	1.372
N6-C10	1.321	1.317	1.315	1.288	1.322	1.319	1.291
C10-N5	1.387	1.380	1.375	1.362	1.381	1.376	1.361
C10-C12	1.475	1.464	1.461	1.476	1.466	1.463	1.477
C12-C17	1.391	1.403	1.400	1.389	1.406	1.403	1.391
C17-C20	1.389	1.388	1.386	1.382	1.391	1.388	1.383
C20-C21	1.383	1.390	1.387	1.379	1.394	1.391	1.381
C21-N8	1.467	1.479	1.473	1.467	1.473	1.468	1.462
N5-H22	0.956	1.006	1.006	0.991	1.008	1.007	0.991
C17-H26	0.986	1.083	1.084	1.074	1.085	1.086	1.074
C20-H29	0.996	1.081	1.082	1.071	1.082	1.083	1.071
Bond angles (°)							
O1-N7-O2	124.35	124.48	124.67	124.60	124.25	124.50	124.50
O1-N7-C15	117.82	117.82	117.72	117.79	117.92	117.82	117.83
O2-N7-C15	117.93	117.69	117.59	117.60	117.81	117.67	117.66
C15-C18-H27	119.91	118.56	118.45	119.10	118.60	118.47	119.11
C15-C13-H23	120.70	120.50	120.41	121.06	120.57	120.48	121.06
C18-C14-C11	119.18	118.22	118.17	118.09	118.21	118.17	118.08
C13-C9-C11	120.30	122.81	122.86	122.78	122.88	122.92	122.08
C13-C9-N5	133.25	132.58	132.56	132.48	132.53	132.53	132.48
C9-N5-C10	108.32	107.25	107.25	106.60	107.28	107.27	106.78
N5-C10-N6	113.62	112.16	112.31	113.13	112.20	112.35	112.89
C10-N6-C11	106.32	105.84	105.65	105.67	105.71	105.53	105.79
N6-C10-C12	125.63	124.23	124.06	124.08	124.16	123.99	123.68
C10-C12-C17	123.62	122.30	122.39	121.54	122.26	123.37	122.10
C12-C17-C20	121.80	120.74	120.67	120.48	120.74	120.66	120.61
C12-C16-C19	118.70	120.58	120.54	120.28	120.59	120.56	120.41
C19-C21-N8	118.30	119.16	119.13	118.79	119.18	119.15	119.04
C21-N8-O4	119.20	117.55	117.46	117.47	117.65	117.53	117.50
O4-N8-O3	122.20	124.88	125.08	125.03	124.68	124.92	124.97
C21-N8-O3	119.12	117.55	117.45	117.48	117.65	117.54	117.52
C21-C19-H28	120.10	119.65	119.57	120.12	119.71	119.65	120.15
Torsional angle (°)							
O1-N7-C15-C13	-	-179.99	179.96	179.67	179.95	179.97	179.99
O1-N7-C15-C18	-	0.0068	-0.045	-0.260	-0.028	-0.0575	-0.004
O2-N7-C15-C13	-	0.0064	-0.035	-0.326	-0.0505	-0.0101	0.003
O2-N7-C15-C18	-	-179.94	179.95	179.73	-0.028	179.96	-179.99
O3-N8-C21-C20	-	179.99	-179.92	-179.93	-179.84	-179.80	179.99
O3-N8-C21-C19	-	-0.007	0.037	-0.135	0.102	0.1433	-0.001
O4-N8-C21-C20	-	-0.0084	0.076	0.106	0.163	0.1487	0.003
O4-N8-C21-C19	-	179.91	-179.95	179.90	-179.89	-179.90	-179.99
N5-C10-C12-C16	-	-179.99	179.95	159.74	174.08	173.61	179.98

Torsional angle (°)	Exp. ^a	B3LYP 6311++ G (d, p)	B3PW91 6311++ G (d, p)	HF 6311++ G (d, p)	B3LYP 6311+ G (d, p)	B3PW91 6311+ G (d, p)	HF 6311+ G (d, p)
N5-C10-C12-C17	-	0.020	-3.126	-20.71	-6.078	-6.582	-0.0193
N6-C10-C12-C16	-	0.0235	-3.0612	-20.28	-5.812	-6.397	-0.0184
N6-C10-C12-C17	-	-179.97	176.85	159.25	174.02	173.40	179.98
C18-C14-C11-N6	-	179.99	179.91	179.71	179.88	179.85	180.00
C15-C13-C9-N5	-	-179.99	179.97	179.59	179.94	179.89	-179.99
H27-C18-C14-C11	-	-180.00	-179.980	-179.88	-179.99	-179.96	-180.00
C10-C12-C16-C19	-	-180.00	-179.92	-179.88	-179.91	-179.88	-179.99
C9-N5-C10-C12	-	-180.00	-179.94	-179.27	-179.84	-179.96	179.99
C17-C20-C21-N8	-	-179.99	-179.98	-179.86	-179.93	-179.94	180.00

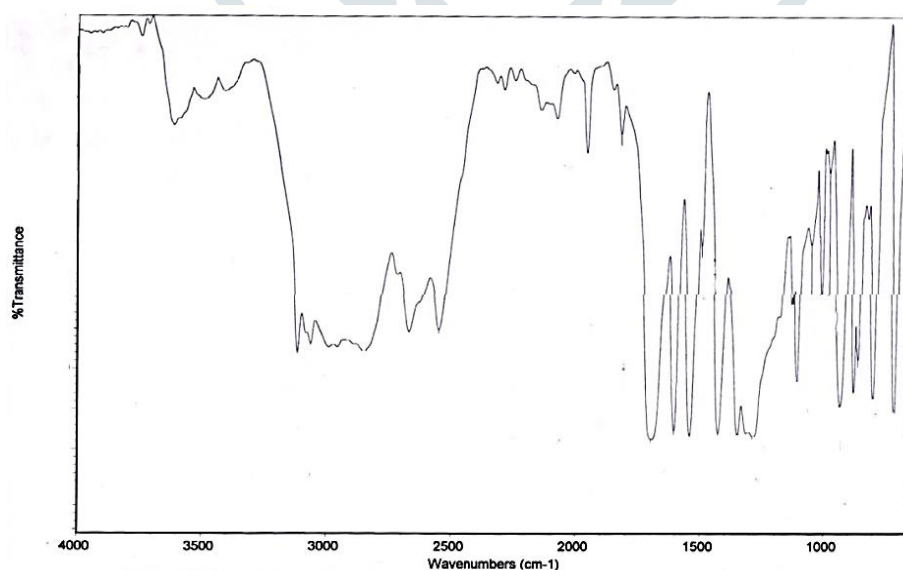
^a Taken from Refs[20-22]

3.2 Vibrational assignments

The theoretical vibrational spectra of 6-nitro-2-(4-nitrophenyl)-1H-benzimidazole were calculated at the HF and DFT (B3LYP/B3PW91) methods with the 6-31+G(d,p) and 6-311++G(d,p) basis sets. FT-IR spectrum was recorded for both the experimental and theoretical methods as presented in the Fig 2. Calculated frequency was scaled with 0.961 for B3LYP, 0.957 for B3PW91 and 0.892 for HF [24] both the frequencies are represented in the Table 2. The vibrational bands assignments have been made by using both the animation option of Gauss view 6.0 graphical interface for Gaussian program 16 W [14] and VEDA 4 program [25]. All the calculated and experimental data are in good agreement.

The FT-IR spectra of the title compound contains some characteristic bands of vibrations such as C-H, N-H, C=N, C-N and C=C, groups. The N-H Stretching occurred in the region of 3518 cm^{-1} [26]. The characteristic vibrations for C-H stretching of heterocyclic aromatic compounds are expected to appear in 3000 and 3100 cm^{-1} [27]. The C-H symmetric stretching vibration of the title compound observed in and around the region of 3100 cm^{-1} for all the DFT and HF basic sets and 3114 cm^{-1} experimentally. The asymmetric C-H was observed at 3061 cm^{-1} experimentally whereas for DFT /B3LYP [6-311++G(d,p)/6-31+G(d,p)] we observed 3098 cm^{-1} / 3117 cm^{-1} for DFT /B3PW91 [6-311++G(d,p)/6-31+G(d,p)] 3092 cm^{-1} / 3112 cm^{-1} and for HF [6-311++G(d,p)/6-31+G(d,p)] 3031 cm^{-1} / 3052 cm^{-1} [28].

The characteristic region of the benzimidazole derivative spectrum is 1500 - 1650 cm^{-1} . The vibrational frequencies and intensity differ in this region based on the substituent and its position [26]. The title compound shows vibrational frequency at 1513 cm^{-1} which is in good agreement with the obtained results. The band appearing at 1596 cm^{-1} and 1313 cm^{-1} are assigned to C=N and C-N [29]. In this study the N-O vibration is observed in the region around 1100 cm^{-1} and in experimental spectrum is 1013 cm^{-1} . The out of bending OCON torsion ONCC and C-C stretching observed at 1105 cm^{-1} , 1046 cm^{-1} and 1011 cm^{-1} . The vibrational spectra of 2-substituted benzimidazole show a very intensive band around the 741 cm^{-1} . The title compound shows C-H and C-C vibration around 790 – 680 cm^{-1} along with their torsion HCCN, bending CCC, bending and torsion HCC is observed in this region.



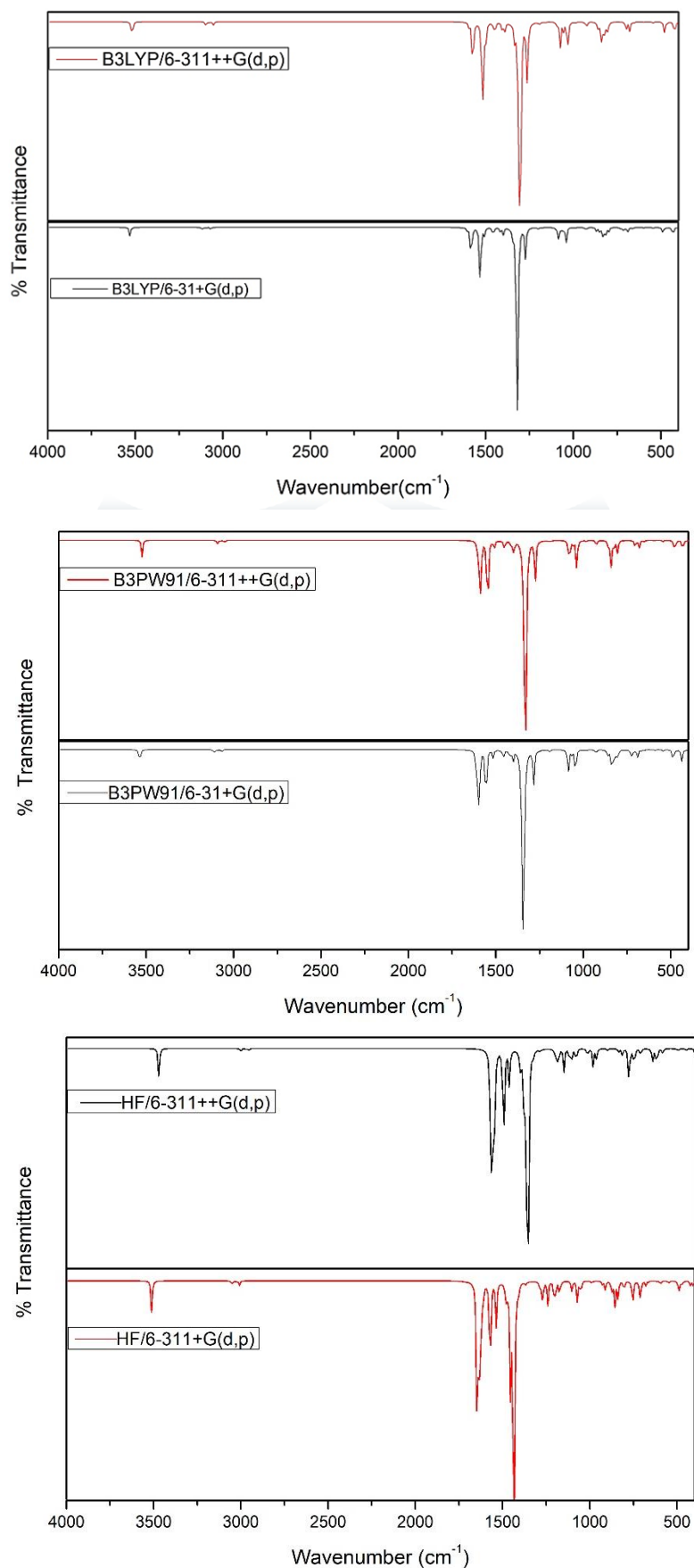


Fig2. The experimental and calculated FT-IR spectra of 6-nitro-2-(4-nitrophenyl)-1H-benzimidazole

Table 2: Experimental and calculated vibrational; frequencies of 6-nitro-2-(4-nitrophenyl)-1H-benzimidazole

Assignments ^a	B3LYP	B3LYP	B3PW91	B3PW91	HF	HF	Exp.
	6311++ G (d, p)	6311+ G (d, p)	6311++ G (d, p)	6311+ G (d, p)	6311++ G (d, p)	6311+ G (d, p)	
$\nu(\text{N-H})$	3518.79	3530.49	3522.60	3536.49	3485.75	3511.35	3613.84
$\nu(\text{C-H})$ s	3100.78	3119.97	3094.71	3114.41	3031.29	3053.13	3114.32
$\nu(\text{C-H})$ as,	3098.88	3117.6	3092.93	3112.38	3031.25	3052.97	3061.87
$\nu(\text{C-H})$ as,	3094.63	3112.41	3089.57	3107.91	3026.07	3046.19	2980.15
$\nu(\text{C=N})$	1596.37	1604.08	1607.03	1613.45	1635.43	1645.78	1698.28
$\nu(\text{C=N})$	1576.75	1585.77	1594.32	1604.13	1625.43	1634.79	1604.29
$\nu(\text{C=C})$	1513.81	1527.48	1543.93	1553.40	1563.81	1571.12	1541.35
$\nu(\text{C-N})$	1313.12	1326.75	1337.90	1349.45	1360.26	1366.51	1349.69
$\nu(\text{C-N})$	1249.76	1255.93	1249.16	1254.94	1197.10	1205.84	1289.22
O-N	1116.93	1109.51	1144.1	1208.46	1240.67	1205.13	1129.71
$\nu(\text{OCON})$	1105.54	1109.51	1090.92	1083.27	1083.52	1075.11	1108.57
$\tau(\text{ONCC})$	1046.09	1048.49	1007.79	1084.27	971.34	971.94	1055.21
$\nu(\text{CC})$	1011.25	1038.48	965.47	966.82	964.91	961.07	1013.4
$\nu(\text{CH}) + \tau(\text{HCCN})$	790.88	790.34	720.21	717.46	711.51	706.49	799.59
$\beta(\text{CCC}) + (\text{CC})$	754.16	744.33	685.01	685.92	680.79	681.83	715.94
$\nu(\text{CH}) + \beta(\text{HCC}) + \tau(\text{HCCC})$	555.87	539.87	502.23	510.98	506.01	502.48	--

ν , stretching; δ , twisting; β , bending; τ , torsion; θ , breathing; s, symmetric; as, asymmetric

3.3 Natural bond orbital (NBO) analysis.

The Natural bond orbital calculation [31] of the 6-nitro-2-(4-nitrophenyl)-1H-benzimidazole was performed using the DFT/B3LYP method with the 6-311++ G (d, p) basis set provided by Gaussian 16 W. NBO analysis is an effective method for studying intra and intermolecular bonding and also provides a convenient basis for investigating charge transfer or conjugative interaction in the molecular systems. The hyper conjugative interaction energy was deduced from the second order perturbation approach of Fock matrix in the NBO basis between electron donor and electron acceptor orbitals [32] and the possible intensive interaction are given in the Table 3. The intensive interaction between the electron donors and electron acceptors can be identified by large E (2) values. The intramolecular hyper conjugative interaction was observed for the bonding orbital σ (C12-C16) which distributes to the anti-bonding orbital σ^* (C16-C19) with the stabilization energy of 65.75 Kcal/mol. The intramolecular hyper conjugative interaction was observed for the bonding orbital σ (C10-C12) which distributes to the anti-bonding orbital σ^* (C16-C19) with the stabilization energy of 32.78 Kcal/mol. The intramolecular hyper conjugative interaction was observed for the bonding orbital σ (C20-H29) which distributes to the anti-bonding orbital σ^* (C15-C18) with the stabilization energy of 188.89 Kcal/mol and for the bonding orbital σ (N8-C21) which distributes to the anti-bonding orbital, σ^* (C15-C18) and σ^* (C16-C19) with the stabilization energy of 59.46 and 158.11 Kcal/mol. The intramolecular hyper conjugative interaction was observed for the bonding orbital σ (O4-N8) which distributes to the anti-bonding orbital σ^* (C15-C18) and σ^* (C16-C19) with the stabilization energy of 37.14 and 94.67 Kcal/mol. The increased occupancy of the localized π (C13-C15) in the idealized non-Lewis structure and decreased occupancy of π (C13-C15) in the idealized Lewis orbital and their subsequent impact on their molecular stability and geometry also related with their pure p character of the two carbons C13 and C15. The intramolecular hyper conjugative interaction was observed for the bonding orbital π (C14-C18), which distributes to the anti-bonding orbital π^* (C13-C15) with the stabilization energy of 20.11 Kcal/mol. This leads to strong stabilization of benzimidazole moiety [33]

Table 3. Significant donor acceptor interaction of 6-Nitro-2-(4-nitrophenyl)-1H-benzimidazole and their second order perturbation energies calculated at B3PW91/6-311++G (d, p) basis set.

Donor Orbital(i)	Type	ED/e	Acceptor orbital (j)	Type	ED/e	E (2) (kcal/mol) ^a	E(j)-E(i) (a.u.) ^b	F(i,j) (a.u.) ^c
O1-N7	σ	1.99566	N7 - C15	σ^*	0.10488	0.84	1.38	0.031
O1-N7	σ	1.99566	C13-C15	σ^*	0.02093	0.63	1.64	0.029
O1-N7	π	1.98549	C13-C15	π^*	0.38497	4.33	0.46	0.044
O2-N7	σ	1.99576	N7-C15	σ^*	0.10488	0.76	1.38	0.03
O2-N7	σ	1.99576	C15-C18	σ^*	0.02249	0.53	1.22	0.023
O3-N8	σ	1.9958	N5-C10	σ^*	0.04258	1.06	1.31	0.034
O3-N8	σ	1.9958	N5-H22	σ^*	0.01847	1.25	1.41	0.038
O3-N8	σ	1.9958	C15-C18	σ^*	0.02249	11.3	1.24	0.106
O3-N8	σ	1.9958	C16-C19	σ^*	0.01454	23.31	0.77	0.12
O4-N8	σ	1.99581	N5-C10	σ^*	0.04258	7.76	1.31	0.091
O4-N8	σ	1.99581	C14-H24	σ^*	0.01342	12.89	1.37	0.119
O4-N8	σ	1.99581	C15-C18	σ^*	0.02249	37.14	1.23	0.192
O4-N8	σ	1.99581	C16-C19	σ^*	0.01454	94.67	0.76	0.24
N5-C9	σ	1.98376	N5-C10	σ^*	0.04258	2.53	1.04	0.046
N5-C9	σ	1.98376	C10-C12	σ^*	0.03737	3.58	1.26	0.06
N5-H22	σ	1.98863	N6-C10	σ^*	0.01435	2.35	1.26	0.049
N6-C10	σ	1.97811	C11-C14	σ^*	0.02359	5.47	1.41	0.078
N7-C15	σ	1.98843	C14-C18	σ^*	0.01216	1.37	1.4	0.039
N8-C21	σ	1.98846	C15-C18	σ^*	0.02249	59.46	0.97	0.215
N8-C21	σ	1.98846	C16-C19	σ^*	0.01454	158.11	0.5	0.25
C9-C11	π	1.55232	C13-C15	π^*	0.38497	21.82	0.28	0.071
C9-C11	π	1.55232	C14-C18	π^*	0.26876	16.16	0.3	0.065
C10-C12	σ	1.97143	C16-C19	σ^*	0.01454	32.78	0.36	0.097
C11-C14	σ	1.97713	C14-C18	σ^*	0.01216	2.61	1.3	0.052
C12-C16	σ	1.97011	C16-C19	σ^*	0.01454	65.75	0.37	0.139
C13-C15	π	1.69595	O1-N7	π^*	0.6253	25.96	0.15	0.061
C14-C18	π	1.70486	C13-C15	π^*	0.38497	20.11	0.27	0.068
C15-C18	σ	1.97499	C14-H24	σ^*	0.01342	2.64	0.98	0.046
C16-H25	σ	1.97728	C16-C19	σ^*	0.01454	13.21	0.18	0.044
C18-H27	σ	1.97485	C14-H24	σ^*	0.01342	0.53	0.79	0.018
C19-H28	σ	1.97514	C12-C16	σ^*	0.02276	3.61	1.06	0.055
C20-H29	σ	1.97512	C15-C18	σ^*	0.02249	188.89	0.64	0.31

^a E⁽²⁾, energy of hyperconjugative interactions.^b Energy difference between donor and acceptor i and j NBO orbitals^c F_{ij} is the Fock matrix element between i and j NBO orbitals

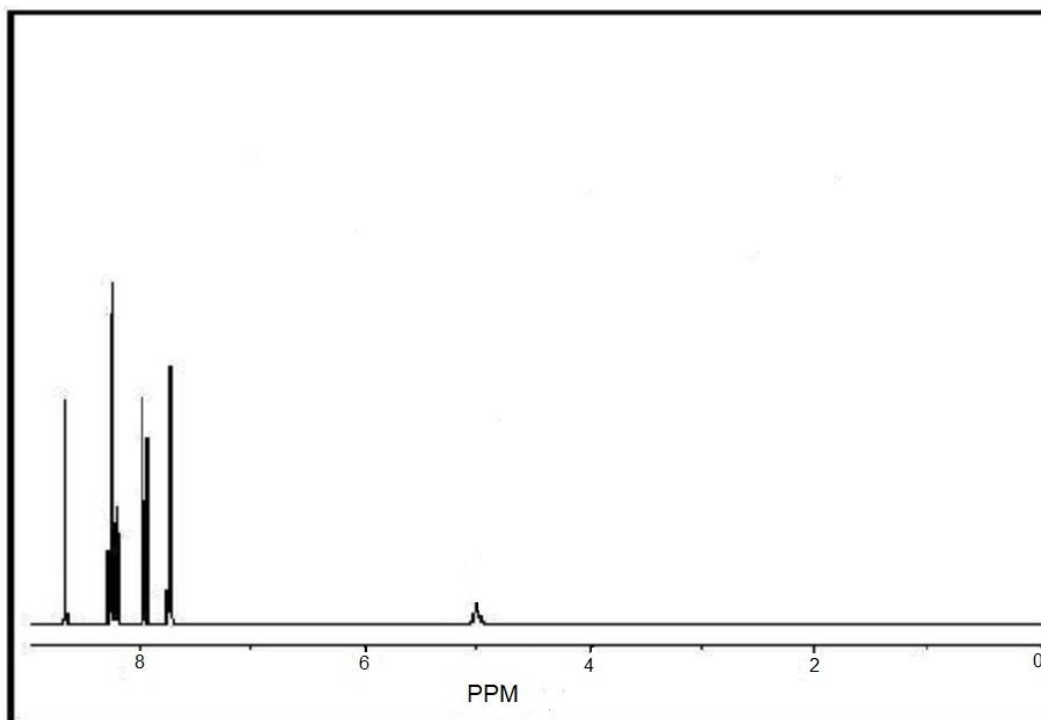
3.4¹H NMR spectra analysis

In order to provide an unequivocal assignment of ¹ H NMR spectra of the 6-nitro-2-(4-nitrophenyl)-1H-benzimidazole compound, we consider series of NMR calculation using GIAO method [30]. All the calculation are performed using DFT/B3LYP method with the 6-311++ G (d, p) basis set and the results are tabulated in the Table 3. The integral equation formalism –polarized continuum model (IEF-PCM) provided by Gaussian 16W is considered to describe the influence exerted by the solvents (DMSO, Ethanol, Chloroform) on the NMR spectra of the given compound and the calculated values are also listed in the Table 4.

The ¹ H NMR experimental chemical shifts of title compound were observed 7.74-8.63 ppm as shown in Fig 3. These chemical shift was calculated at 7.79-9.2 ppm for DMSO, 7.77-9.25 ppm for ethanol and 7.55-9.24 ppm for chloroform. Thus the GIAO method shows the significant difference in chemical shift in the Table 3, with respect to experimental and theoretical evaluation. It was observed that the chemical shifts in all solvents are almost equal.

Table 4. Experimental and calculated (GIAO)¹H NMR chemical shifts for of 6-nitro-2-(4-nitrophenyl)-1H-benzimidazole.

Atom	Exp.	B3LYP/6-311++G(d,p)		
¹ H		DMSO	Ethanol	Chloroform
H23	8.63	8.5406	8.5267	8.4225
H24	7.96	8.0997	8.0981	8.0775
H25	7.74	8.8796	8.8815	8.8898
H26	7.74	8.108	8.0935	7.9796
H27	8.19	8.3656	8.3693	8.3930
H28	8.25	9.2604	9.2596	9.2481
H29	8.25	7.9966	7.9935	7.9685

**Fig 3.** ¹H- NMR spectra of 6-nitro-2-(4-nitrophenyl)-1H-benzimidazole

3.5 Electronic properties

The electronic transition of 6-nitro-2-(4-nitrophenyl)-1H-benzimidazole were calculated using B3LYP/6-311++G (d, p) basis set of DFT in gas phase and in solvents such as DMSO, Chloroform and water. The effect of solvent was evaluated by applying the integral equation formalism of the polarizable continuum model (IEF-PCM). The UV-vis spectral data for both the gas and solvents phase were illustrated in Table 5, by using Gausssum3.0 [34]. The absorption wavelength values in the UV study of the title compound are almost equal in both the gas and solvents phase. According to calculated electronic data shows the absorption band in the range of 300-430 nm in all the states. We know very well that the $n \rightarrow \pi^*$ transition is not seen in benzimidazole compound but it has a lone pair of electron on nitrogen atom [35-36]. The broad band we observed is due to the $\pi \rightarrow \pi^*$ transition in the benzimidazole ring. The longest wavelength corresponding to electronic transition from HOMO to the LUMO (74%) and the wavelength is 423 nm for gas whereas for DMSO HOMO to the LUMO (96%) and the wavelength is 417 nm, chloroform HOMO to the LUMO (93%) and the wavelength is 408 nm and for water HOMO to the LUMO (95%) and the wavelength is 416 nm. The large λ indicates that more electrons are pushed into the aromatic ring structure.

The energies of the frontier molecular orbitals (FMOs) for the title compound are shown in Figure 4. We had found the HOMO and LUMO energies and the energy gap (ΔE), the ionization potential (I), the electron affinity (A), the electronegativity (χ), global hardness (η), global softness (S) and the Electrophilicity index (ω) for the title compound have been calculated using B3LYP/6-311++G(d,p) basis set. The HOMO-LUMO energy gap is very important parameter for the stability of the structure [37] and also it reflect the biological activity of the compound. The energy value of the band gap is 3.4155 eV for HOMO to LUMO and 3.7232 for HOMO to LUMO +1. This ensure that the compound is stable. The global hardness is another good indicator of chemical stability. The global hardness of the title compound is 1.7075 as shown in Table 6, which indicates the good chemical stability and the compound is stable, electronegativity (χ) is calculated as 5.5157 which is a measure of attraction of an atom to electron. The extremely low global softness of 0.2928 theoretical value shows the compound is nontoxic. The Electrophilicity index (ω) was found to be 8.9086 this ensures that there is strong energy transformation between HOMO and LUMO, this electrophilicity index act as a pre-cursor to analyze the biological activity in terms of docking where the title compound act as ligand and it is docked to a suitable protein [38].

Table 5. Calculated electronic transition states for the 6-nitro-2-(4-nitrophenyl)-1H-Benzimidazole with the TD-DFT/IEF-PCM method.

	DFT/B3LYP with 6-311++G (d,p)				
	λ (nm)	Band gap (eV)	Oscillator Strength	Major contributions	
Gas	423	2.9284	0.0000	HOMO-3->LUMO (74%),	HUMO-3->LUMO+1 (21%)
	421	2.9458	0.0003	HOMO-2->LUMO (37%),	HUMO-2->LUMO+1 (59%)
	378	3.2814	0.6044	HOMO->LUMO (97%),	
	344	3.6074	0.0389	HOMO-1->LUMO (29%),	HOMO->LUMO+1 (58%)
	335	3.6978	0.1032	HOMO-1->LUMO (62%),	HOMO->LUMO+1 (35%)
	317	3.9105	0.0005	HOMO-10->LUMO (72%),	HOMO-10->LUMO+1(21%)
DMSO	417	2.9718	0.6595	HOMO->LUMO (96%)	
	397	3.1239	0.0003	HOMO-4->LUMO (70%),	HOMO-4->LUMO+1 (26%)
	393	3.1534	0.002	HOMO-3->LUMO (41%),	HOMO-3->LUMO+1 (55%)
	380	3.2650	0.0722	HOMO-1->LUMO (20%),	HOMO->LUMO+1 (67%)
	364	3.4092	0.1217	HOMO-1->LUMO (69%),	HOMO->LUMO+1 (26%)
	348	3.5670	0.0992	HOMO-2->LUMO (69%),	HOMO-1->LUMO+1 (21%)
Chloroform	408	3.0383	0.6743	HOMO->LUMO (93%)	
	404	3.0679	0.0081	HOMO-4->LUMO (70%),	HOMO-4->LUMO+1 (25%)
	401	3.0929	0.0165	HOMO-3->LUMO (40%),	HOMO-3->LUMO+1 (55%)
	370	3.3516	0.0619	HOMO-1->LUMO (21%),	HOMO->LUMO+1 (67%)
	356	3.4816	0.1203	HOMO-1->LUMO (69%),	HOMO->LUMO+1 (27%)
	338	3.6695	0.087	HOMO-2->LUMO (68%),	HOMO-1->LUMO+1 (22%)
Water	416	2.9773	0.6354	HOMO->LUMO (95%)	
	396	3.1271	0.0003	HOMO-4->LUMO (70%),	HOMO-4->LUMO+1 (26%)
	393	3.1570	0.002	HOMO-3->LUMO (41%),	HOMO-3->LUMO+1 (55%)
	380	3.2646	0.073	HOMO-1->LUMO (20%),	HOMO->LUMO+1 (67%)
	364	3.4094	0.1201	HOMO-1->LUMO (69%),	HOMO->LUMO+1 (27%)
	348	3.5647	0.1006	HOMO-2->LUMO (69%),	HOMO-1->LUMO+1 (21%)

Table 6. Global chemical reactivity descriptors of 6-nitro-2-(4-nitrophenyl)-1H-benzimidazole

Properties	B3LYP/6-311++G(d,p)
E_{HOMO} (eV)	-7.2232
E_{LUMO} (eV)	-3.8082
Ionisation potential (I)	7.2232
Electron affinity(A)	3.8082
Chemical potential (μ)	-5.5157
Electronegativity (χ)	5.5157
Global hardness(η)	1.7075
Global softness (S)	0.2928
Electrophilicity index (ω)	8.9086

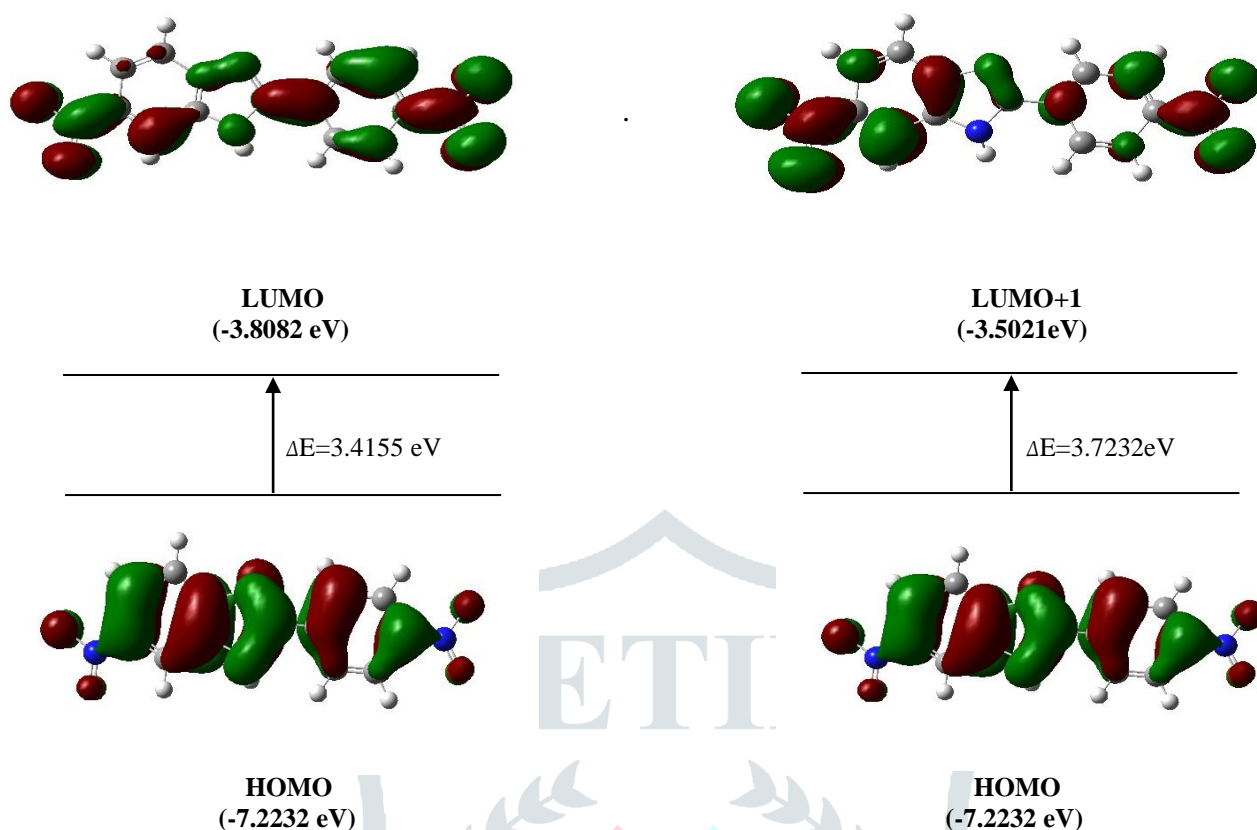


Fig 4. The molecular orbital of 6-nitro-2-(4-nitrophenyl)-1H-benzimidazole using DFT/B3LYP with 6-311++G (d, p) and the selected electronic transition in DMSO phase

3.6 Molecular electrostatic potential (MEP)

Molecular electrostatic potential is associated to the electron density and is a very useful descriptor in discerning sites for electrophilic and nucleophilic reactions as well as hydrogen bonding interactions [39-40]. The electrostatic potential is a real physical property, which can be determined experimentally as well as computationally [41]. MEP map was generated to predict the reactive sites for electrophilic and nucleophilic attack. It is generated using the optimized geometry of the 6-nitro-2-(4-nitrophenyl)-1H-benzimidazole by DFT/B3LYP with 6-311++G (d, p) basis set using Gauss View 6.0 program. The red colour (negative) region represents the electrophilic reactivity and the blue colour (positive) region represents the nucleophilic reactivity as shown in Fig 5. It can be seen from the figure negative region is localized near the nitrogen atom of the benzimidazole ring and the maximum positive region is associated with the H atoms of the imidazole indicating possible site for nucleophilic attack. This result extends information about the intermolecular interaction and molecular bonding.

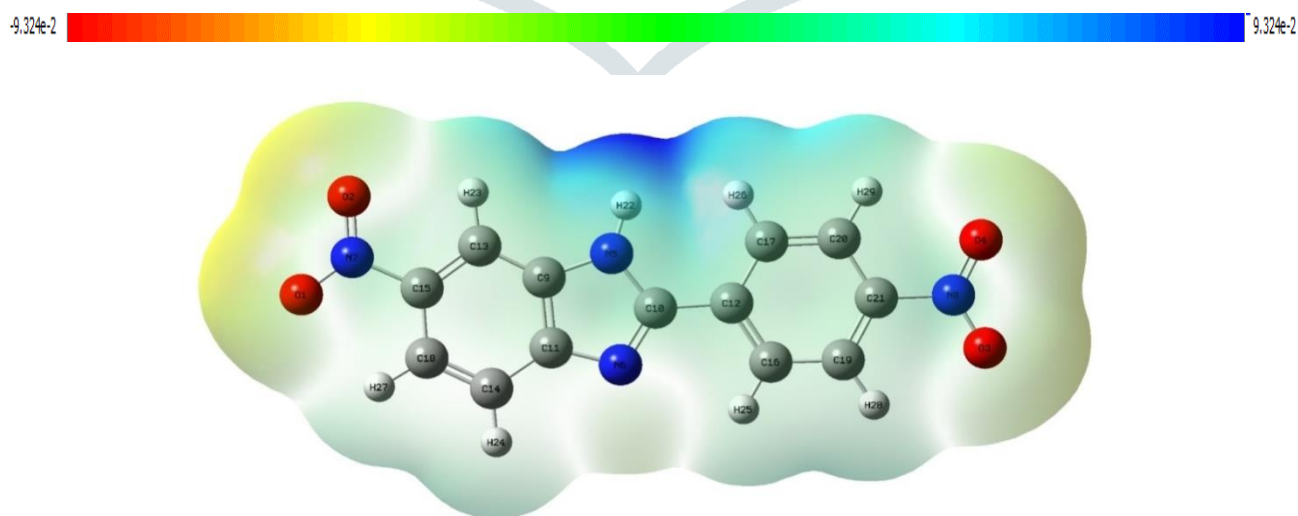


Fig 5. The molecular electrostatic potential of 6-nitro-2-(4-nitrophenyl)-1H-benzimidazole using DFT/B3LYP with 6-311++G (d, p)

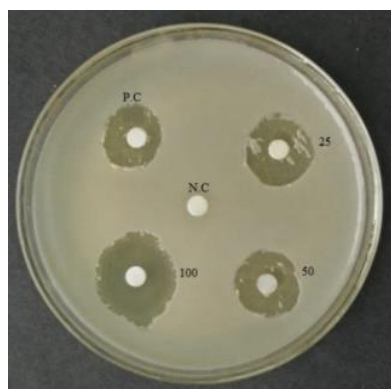
3.7 Anti-microbial activity:

The antimicrobial activities were carried for total of four bacterial strains viz. *Staphylococcus aureus* (MTCC-3160), *Enterococcus faecalis* (MTCC-3159) as Gram –positive bacteria and *Pseudomonas aeruginosa* (MTCC-4030), *Escherichia coli* (MTCC-1667) as Gram-negative bacteria and two fungal strains viz. *Aspergillus niger* (MTCC 282), *Candida albicans* (MTCC 227) were used in the investigation. They were chosen based on their clinical and pharmacological importance. The bacterial and fungal strains obtained from Microbial Type Culture Collection, Institute of Microbial Technology, Chandigarh, were used for evaluating antimicrobial activity. The bacterial strains were grown in Mueller-Hinton agar (MHA), whereas the fungal strains were grown in potato dextrose agar. Antimicrobial activity of 6-nitro-2-(4-nitrophenyl)-1H-benzimidazole compound was determined by Disc diffusion method according to National Committee for Clinical Laboratory Standards (NCCLS). Inoculum of each microbial culture to be tested was spread on agar plates with a sterile swab moistened with the microbial suspension. Subsequently, discs of 6 mm diameter were kept into the agar medium and filled with 20 µl (25, 50, 100 µg/ml) of 6-nitro-2-(4-nitrophenyl)-1H- benzimidazole compound and allowed to diffuse at room temperature for 2 h. The plates were then incubated in the upright position at 37°C for 24 h for bacterial culture and 28°C for 48 h for fungal culture. Disc containing the same volume of ethanol served as negative controls while standard antibiotic Ciprofloxacin 25 mg (50 µl) were used as the positive controls. After incubation, the growth inhibition zones were measured in mm dia. Three replicates were carried for a compound against each of the test organism. Data were expressed as mean \pm standard deviation.

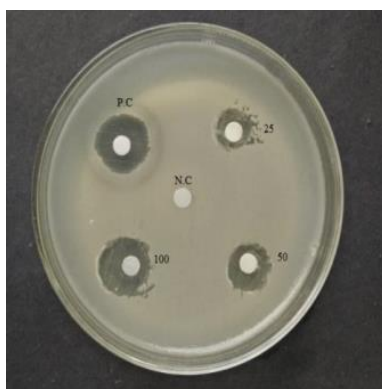
The zone of inhibition ranged from 20 \pm 2.4 to 29 \pm 3.4, 10 \pm 1.1 to 20 \pm 2.2, 17 \pm 1.5 to 23 \pm 2.1, 13 \pm 1.1 to 23 \pm 1.8, 18 \pm 1.9 to 29 \pm 3.1 and 14 \pm 1.2 to 24 \pm 2.1 are in mm diameter for *Staphylococcus aureus*, *Enterococcus faecalis*, *Pseudomonas aeruginosa*, *Escherichia coli*, *Aspergillus niger* and *Candida albicans*. This indicates the diameter increases with increase in concentration of the title compound. Maximum activity was shown against *Staphylococcus aureus* and *Aspergillus niger* with inhibitory zone of 20 \pm 2.4 to 29 \pm 3.4 and 18 \pm 1.9 to 29 \pm 3.1 at the concentration of 100 µg/ml whereas least activity was shown against *Enterococcus faecalis* (10 \pm 1.1 to 20 \pm 2.2). From the Table 7 it clearly indicates that the 6-nitro-2-(4-nitrophenyl)-1H-benzimidazole compound has the capacity of inhibiting the metabolic growth of the investigated bacteria and fungi to some extent especially *Staphylococcus aureus* and *Aspergillus niger* as shown in fig 6. It is well evident that most number of drugs would be active against Gram-positive than Gram-negative bacteria [42]. In this present study the title compound as shown that it is active against both types of the bacteria and fungi, which may indicate broad spectrum of properties this remarkable activity of this title compound may be arising from the benzimidazole ring, which plays an vital role in the anti-microbial activity [43] and also due to nitro group attached to the benzimidazole ring hence it is noted that there is direct relationship between the biological activity and electron withdrawing group [44]. However the title compound shows the lower antimicrobial potencies than the compared control drug except in *Staphylococcus aureus* which is also providing the little higher activity than the compared control drug. It is evident from this work that some more exploration of benzimidazole derivative at the para position will lead to development of the some very potent antimicrobial agent.

Table 7 : Antimicrobial activity of the 6-nitro-2-(4-nitrophenyl)-1H-benzimidazole by Disc diffusion method

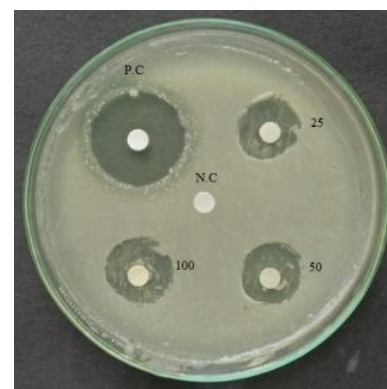
Microbial Compound	Diameter of the Inhibition Zone (mm)			
	25 µg/ml	50 µg/ml	100 µg/ml	Ciprofloxacin 25µg/ml
Gram Positive				
<i>Staphylococcus aureus</i> (MTCC-3160)	20 \pm 2.4	23 \pm 2.7	29 \pm 3.4	19 \pm 2.2
<i>Enterococcus faecalis</i> (MTCC-3159)	10 \pm 1.1	14 \pm 1.5	20 \pm 2.2	18 \pm 1.9
Gram -Negative				
<i>Pseudomonas aeruginosa</i> (MTCC-4030)	17 \pm 1.5	19 \pm 1.7	23 \pm 2.1	29 \pm 2.6
<i>Escherichia coli</i> (MTCC-1667)	13 \pm 1.1	20 \pm 1.6	23 \pm 1.8	39 \pm 3.1
Fungal Compound				
<i>Aspergillus niger</i> (MTCC 282),	18 \pm 1.9	26 \pm 2.8	29 \pm 3.1	27 \pm 2.9
<i>Candida albicans</i> (MTCC 227)	14 \pm 1.2	18 \pm 1.6	24 \pm 2.1	16 \pm 1.4



Staphylococcus aureus



Enterococcus faecalis



Pseudomonas aeruginosa

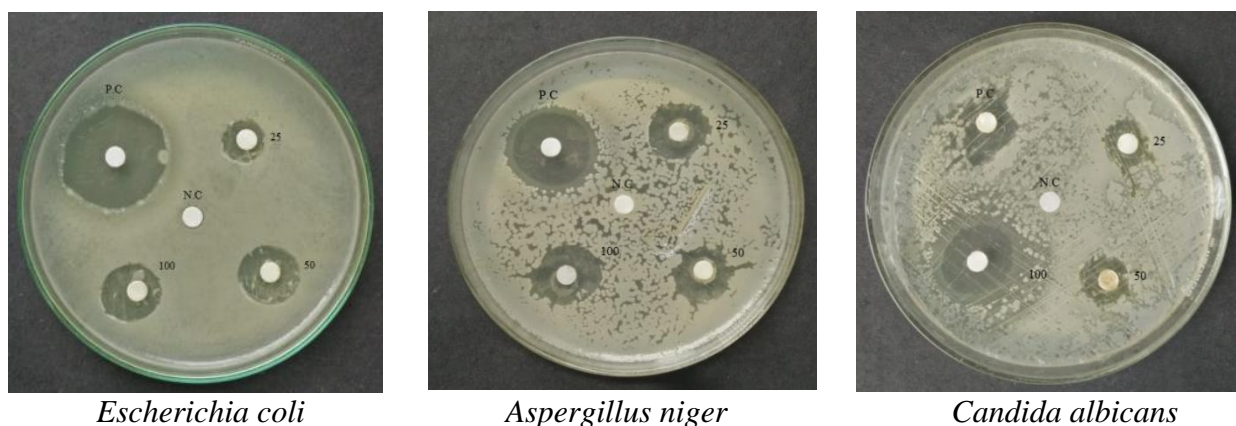


Fig 6. Anti-bacterial activity of the 6-nitro-2-(4-nitrophenyl)-1H-benzimidazole

4. CONCLUSION

In this study we synthesized the 6-nitro-2-(4-nitrophenyl)-1H-benzimidazole compound. We thoroughly investigated the FT-IR spectra, UV- vis, ^1H proton NMR, Natural Bond Orbital (NBO) and Molecular Electrostatic Potential (MEP) in detail manner for the first time. The calculated geometrical parameter are in good agreement with the literature data. A FT-IR spectra analysis shows that the calculated vibrational frequencies are in good agreement with the experimental values. From NBO analysis, the intermolecular interaction and the stabilization energy have been determined. The chemical shifts values for different solutions were determined and compared with experimental data which shows a very good agreement for ^1H Proton NMR. The energy gap of 3.4155 eV of the present compound and electrophilicity index value was determined using HOMO and LUMO energies. The high electrophilicity index value indicates that the title compound is biological active. The MEP map indicates that the hydrogen atom attached to the benzimidazole ring is more positive. These sites give us the information about the intermolecular interaction and the metallic bonding of the title compound. The synthesized compound is screened for antimicrobial activity against the bacteria and fungi. This compound has shown moderate activity against the entire gram positive and gram negative bacteria and fungi except *Staphylococcus aureus* where it shows comparable highly active then the reference compound. The present study has revealed the antibacterial activity of the title compound and it can also be seen as potential source of useful drugs. Further studies have to be carried out by substituting the electron withdrawing group at the different position of the benzimidazole ring for further enhancement of the antimicrobial activity.

Acknowledgement

The authors are thankful to the UGC for providing financial support under the scheme of “Minor Research Projects” in carrying out this work.

References:

1. Z. Chen, S. Q. Li, W. L. Liao, Z. G. Xie, M. S. Wang, Y. Cao, J. Zhang, Z. G. Xu, Efficient method for the synthesis of fused benzimidazole-imidazoles via deprotection and cyclization reactions, *Tetrahedron*. 71 (2015) 8424-8427.
2. C. S. Digwal, U. Yadav, A. P. Sakla, P. V. S. Ramya, S. Aaghaz, A. Kamal, VOSO₄ catalyzed highly efficient synthesis of benzimidazoles, benzothiazoles, and quinoxalines, *Tetrahedron. Lett.* 57 (2016) 4012-4016.
3. T. Sakai, T. Hamada, N. Avada, J. Watanabe, *Pharmabiol. Dyn.* 12 (1989) 530.
4. C. W. Evans, C. Atkins, A. Pathak, B. E. Gilbert, J. W. Noah, Benzimidazole analogs inhibit respiratory syncytial virus G protein function, *Antiviral. Res.* 121 (2015) 31-38.
5. M. Hranjec, G. Pavlovic, G. K. Zamola, Synthesis, crystal structure determination and antiproliferative activity of novel 2-amino-4-aryl-4,10-dihydro[1,3,5]triazino[1,2-a]benzimidazoles, *J. Mol. Struct.* 1007 (2012) 242-251.
6. M. C. Sharma, S. Sharma, N. K. Sahu, D. V. Kohli, 3D QSAR kNN-MFA studies on 6-substituted benzimidazoles derivatives as non-peptide angiotensin II receptor antagonists: A rational approach to Anti-hypertensive agents, *J. Saudi. Chem. Soc.* 17 (2013) 167-176.
7. A. T. Mavrova, D. Wesselinova, N. Vassilev, J. A. Tsenov, Design, synthesis and antiproliferative properties of some new 5-substituted-2-iminobenzimidazole derivatives, *Eur. J. Med. Chem.* 63 (2013) 696-701.
8. C. G. Opez, F. V. Albores, V. G. Prieto, M. Ruocco, M. Lorito, Changes in *Trichoderma asperellum* enzyme expression during parasitism of the cotton root rot pathogen *Phymatotrichopsis omnivora*, *Fungal. Biol.* 119 (2015) 264-273.
9. Z. Zhang, K. K. Ojo, S. M. Johnson, E. T. Larson, P. H. J. A. Geiger, A. C. Gonzalez, A. C. White, M. Parsons, E. A. Merritt, D. J. Maly, C. L. M. J. Verlinde, W. C. V. Voorhis, E. Fan, Benzoylbenzimidazole based selective inhibitors targeting *Cryptosporidium parvum* and *Toxoplasma gondii* calcium-dependent protein kinase-1, *Bioorg. Med. Chem. Lett.* 22 (2012) 5264-5267.
10. S. Dhole, M. Selvaraju, B. Maiti, K. Chanda, C. M. Sun, Microwave controlled reductive cyclization: a selective synthesis of novel benzimidazole-alkoxy pyrrolo[1,2-a]quinoxalinones, *ACS Comb. Sci.* 17 (2015) 310-316.
11. Singh J, Grover P, Pathak DP. Synthesis and Comparative QSAR study of some novel benzimidazole derivatives. *Acta. Pharm. Sci.* (2010) 52: 510-521.
12. M. Sugumaran, M. Yokes Kumar, Synthesis and Biological Activity of Novel 2, 5 Disubstituted Benzimidazole Derivatives *International Journal of Pharmaceutical Sciences and Drug Research* 2012; 4(1): 80-83
13. M. J. Frisch, G. W. Trucks, H. B. Schlegel, G. E. Scuseria, M. A. Robb, J. R. Cheeseman, G. Scalmani, V. Barone, G. A. Petersson, H. Nakatsuji, X. Li, M. Caricato, A. V. Marenich, J. Bloino, B. G. Janesko, R. Gomperts, B. Mennucci, H. P. Hratchian, J. V. Ortiz, A. F. Izmaylov, J. L. Sonnenberg, D. Williams-Young, F. Ding, F. Lipparini, F. Egidi, J. Goings, B. Peng, A. Petrone, T. Henderson, D. Ranasinghe, V. G. Zakrzewski, J. Gao, N. Rega, G. Zheng, W. Liang, M. Hada, M. Ehara, K. Toyota, R. Fukuda, J. Hasegawa, M. Ishida, T. Nakajima, Y. Honda, O. Kitao, H. Nakai, T. Vreven, K. Throssell,

- J. A. Montgomery, Jr., J.E. Peralta, F. Ogliaro, M. J. Bearpark, J. J. Heyd, E. N. Brothers, K. N. Kudin, V. N. Staroverov, T. A. Keith, R. Kobayashi, J. Normand, K. Raghavachari, A. P. Rendell, J. C. Burant, S. S. Iyengar, J. Tomasi, M. Cossi, J. M. Millam, M. Klene, C. Adamo, R. Cammi, J. W. Ochterski, R. L. Martin, K. Morokuma, O. Farkas, J. B. Foresman, and D. J. Fox, Gaussian 16, Revision B.01 Gaussian, Inc., Wallingford CT, 2016.
14. Roy Dennington, Todd A. Keith, and John M. Millam, Gauss view Version 6. Semichem Inc., Shawnee Mission, KS, 2016.
 15. C. Moller, M.S. Plesset, Phys. Rev. 46 (1934) 618.
 16. A.D. Becke, J. Chem. Phys. 98 (1993) 5648
 17. C. Lee, W. Yang, R.G. Parr, Phys. Rev. B 37 (1988) 785.
 18. P. Perdew, Y. Wang, Phys. Rev. B 45 (1992) 244
 19. J. Tomasi, B. Mennucci, R. Cammi, Quantum mechanical continuum solvation models, Chem. Rev. 105 (2005) 2999-3094.
 20. Namik O' zdemir, Bilge eren, Muharrem dincer, Yunus Bekdemir. Quantum-Chemical, IR, NMR, and X-ray Diffraction Studies on 2-(4-Chlorophenyl)-1-methyl-1H-benzo[d]imidazole, International journal of Quantum Chemistry. Vol 111(2011), 3112-3124
 21. Olga V. Dorofeeva et al. Molecular structure and conformation of nitrobenzene reinvestigated by combined analysis of gas-phase electron diffraction, rotational constants, and theoretical, Struct Chem (2007) 18:739–753
 22. Rajendran Gandhimathi et al. Geometry optimization, HOMO and LUMO energy, molecular electrostatic potential, NMR, FT-IR and FT-Raman analyses on 4-nitrophenol, Eur. Phys. J. Appl. Phys. (2015) 69: 10202
 23. Hakan Arslan, Öztekin Algül Theoretical Studies of Molecular Structure and Vibrational Spectra of 2-Ethyl-1H-benzo[d]imidazole, Asian Journal of Chemistry Vol. 19, No. 3(2007), 2229-2235
 24. J.P. Merrick, J.D. Moran, L. Radom, J. Phys. Chem. A 111 (2007) 11683-11700
 25. M.H. Jamroz, Vibrational Energy Distribution Analysis VEDA-4, Warsaw, 2004.
 26. D.J. Rabiger, M.M. Joullie, J. Org. Chem. 29 (1964) 476.
 27. M. Evecen, H. Tanak, Material science-Poland 34, (2016), 886-904.
 28. Hakan Arslan, Öztekin Algül Vibrational spectrum and assignments of 2-(4-methoxyphenyl)-1H-benzo[d]imidazole by ab initio Hartree-Fock and density functional methods Spectrochimica Acta Part A 70 (2008) 109–116.
 29. N. Sundaraganesan, S. Ilakiamani, P. Subramani, B.D. Joshua, Spectrochim. Acta Part A 67 (3–4) (2007) 628.
 30. F.J. Luque, J.M. Lopez, M. Orozco, Perspective on Electrostatic interactions of a solute with a continuum. A direct utilization of ab initio molecular potentials for the prediction of solvent effects, Theor. Chem. Acc. 103 (2000) 343–345.
 31. F. Weinhold, J.E. Carpenter, The Structure of Small Molecules and Ions, Plenum, New York 1988, pp. 227
 32. I. Fleming, molecular Orbitals and Organic Chemical Reactions, Wiley, London, 2010.
 33. Nour T. Abdel Ghani, Ahmed M. Mansour, Molecular structure of 2-chloromethyl-1H-benzimidazole hydrochloride: Single crystal, spectral, biological studies, and DFT calculations, Spectrochimica Acta Part A 86 (2012) 605–613
 34. N.M.O. Boyle, A.L. Tenderholt and K.M. Langner, Gaussian 3.0 J. Comp. Chem. 29 (2008), 839-845.
 35. M. Krishnamurthy, P. Phaniraj, S.K. Dogra, Absorptiometric and fluorimetric study of solvent dependence and prototropism of benzimidazole homologues, J. Chem. Soc. Perkin Trans. II (1986) 1917-1925.
 36. A.K. Mishra, S.K. Dogra, Photoluminescence of 2-(o-aminophenyl) benzimidazole, J. Photochem. 31 (1985) 333-344.
 37. R.G. Pearson, Absolute electronegativity and hardness correlated with molecular orbital theory, Proc. Natl. Acad. Sci. 83 (22) (1986) 8440–8441.
 38. H. Tandon, A. Shalini, T. Chakraborty, Molecular electrophilicity index-a promising descriptor for predicting toxicological property, J. Bioequiv. Availabl. 9 (6) (2017) 518–527.
 39. Luque, F. J.; Lopez, J. M.; Orozco, M. Theor Chem Acc 2000, 103, 343-345.
 40. Okulik, N.; Jubert, A. H. Internet Electron. J. Mol Des 2005, 4, 17-30.
 41. Politzer, P.; Truhlar, D. G., Eds. Chemical Applications of Atomic and Molecular Electrostatic Potentials; Plenum Press: New York, 1981.